Magnetic long-range order in the t-J model with finite doping

Hiroyuki Mori*
Department of Physics, Indiana University, Bloomington, Indiana 47405

Minoru Hamada
Department of Materials Science, Faculty of Science, Hiroshima University, Higashi-Hiroshima 724, Japan
(Received 30 November 1992; revised manuscript received 19 May 1993)

The spiral phase of the two-dimensional t-J model and the t-t'-J model is studied in the $S \to \infty$ limit and in the low-doping limit. By rewriting the model in a form that is more transparent for analyzing the carrier-spin interaction, we show that a wave vector characterizing spiral long-range order in the t-J model varies linearly with hole density δ. If we dope more holes, the spiral phase changes discontinuously towards a ferromagnetic phase, the Nagaoka state, at a critical hole density $\delta_c = 3(1+\sqrt{2})J/8t$. The spiral phase, however, does not maintain its stability because of electron-density fluctuations. The next-nearest-neighbor hopping t' stabilizes the Néel phase and allows it to occupy a finite area in the magnetic phase diagram. We also investigate the effect of spiral-spin fluctuations upon the stability of the spiral phase, and find that the stability is not recovered by the spin fluctuations.

I. INTRODUCTION

The physical nature of a doped antiferromagnet on a square lattice is considered to be one of the crucial issues in theoretically clarifying the mechanism of high-temperature superconductivity. One model which is extensively studied in this context is the t-J model:

$$H_{t\text{-}J} = -t \sum_{\langle i,j\rangle,\sigma} \tilde{c}^{\dagger}_{i\sigma}\tilde{c}_{j\sigma} + \text{H.c.} + J\sum_{\langle i,j\rangle} \mathbf{S}_i \cdot \mathbf{S}_j, \qquad (1)$$

where $\tilde{c}_{i\sigma} = c_{i\sigma}(1 - n_{i,-\sigma})$. At half filling, the t term vanishes as a result of the constraint of no double occupancy at each lattice site, and the model becomes that of a Heisenberg antiferromagnet, which is believed to have a Néel ordered ground state. Upon introducing holes at half filling, the magnetic structure may be significantly modified because the holes prefer ferromagnetic surroundings in order to propagate smoothly. So far, several studies[1–4] have suggested that the Néel order becomes incommensurate upon doping. Shraiman and Siggia[1] semi-phenomenologically showed that doping induces a spiral state where the staggered magnetization rotates in a plane with a wave vector proportional to the electron number density. Kane *et al.*,[2] Auerbach and Larson,[3] and Igarashi and Fulde[4] obtained similar results using the slave-fermion technique. Auerbach and Larson,[3] however, pointed out that the spiral phase is not stable owing to the negative compressibility of electrons. The spiral order and its instability against density fluctuations are also present in the large-U Hubbard model near half filling.[5,6] Schultz[6] showed that the spiral pitch varies with the hole density and continuously becomes that of Nagaoka ferromagnetism.

In this paper we obtain qualitatively similar results for the t-J model using a different and more physically transparent technique. We also study the spiral-spin wave effect on the coherent hole motion.

From now on we shall work units such that $\hbar = 1$ and the lattice constant $a = 1$.

II. SPIRAL ORDER

We begin the analysis by rewriting the t-J model into a form more convenient to handle the interaction between carrier hopping and the spin structure. Noting that $\tilde{c}_\sigma = c_{-\sigma}S^{-\sigma}$, $\sigma\tilde{c}_\sigma = 2c_\sigma S^z$, and $0 = c_\sigma S^{-\sigma}$, where S^σ is defined by $S^+ = c^{\dagger}_{\uparrow}c_{\downarrow}$ when $\sigma = 1$ and $S^- = c^{\dagger}_{\downarrow}c_{\uparrow}$ when $\sigma = -1$, we can easily show that the t-J Hamiltonian (1) takes the form

$$H_{t\text{-}J} = -\frac{4}{3}t \sum_{\langle i,j\rangle,\sigma} \mathbf{S}_i c^{\dagger}_{i\sigma}c_{j\sigma}\mathbf{S}_j + \text{H.c.} + J\sum_{\langle i,j\rangle} \mathbf{S}_i \cdot \mathbf{S}_j. \quad (2)$$

We note that Eq. (2) is a rotationally symmetric form of the Hamiltonian studied by Xu *et al.*,[7] who analyzed hole motion in the Néel background. The t term of Eq. (2) explicitly shows the coupling of carrier hopping and spins.

In order to study the spiral-spin structure, it is useful to rotate the coordinates at each site. We rotate them at an i site about the y axis by an angle $\theta_i = \mathbf{q}\cdot\mathbf{r}_i$. In the new frame we assume ferromagnetic long-range order (LRO), which corresponds in the original frame to spiral LRO with wave vector $\mathbf{q}$. We omit the degrees of freedom of the particles with down spin in the rotated coordinates, which means that no spin fluctuation is considered at this stage, that is, we use the $S \to \infty$ limit approximation. Then the t-J Hamiltonian is written as

$$H = -\frac{4}{3}t\sum_{\langle i,j\rangle} S^2 \cos\mathbf{q}\cdot(\mathbf{r}_i-\mathbf{r}_j)\cos\frac{\mathbf{q}}{2}\cdot(\mathbf{r}_i-\mathbf{r}_j)d_i^\dagger d_j + \text{H.c.} + J\sum_{\langle i,j\rangle} S^2\cos\mathbf{q}\cdot(\mathbf{r}_i-\mathbf{r}_j), \tag{3}$$

where d represents the up-spin-particle operator $d_\uparrow$ defined in the rotated coordinates, and $d_\downarrow$ is omitted. Notice that the Hamiltonian (3) is valid only in the low-doping limit since the J term must be modified if a moderate density of holes is doped. Transforming Eq. (3) into momentum space, we obtain

$$H = -\frac{8}{3}tS^2\sum_{\mathbf{k}}(C_{q_x}C_{q_x/2}C_{k_x} + C_{q_y}C_{q_y/2}C_{k_y})d_{\mathbf{k}}^\dagger d_{\mathbf{k}} + JS^2N(C_{q_x}+C_{q_y}), \tag{4}$$

where we write $\cos q$ as C_q in short. In the half-filled case, $\langle d_i^\dagger d_i\rangle = 1$, the hopping term does not contribute to the energy, and the total energy has a minimun at $\mathbf{q} = (\pm\pi,\pm\pi)$. This is just a classical result for the Heisenberg antiferromagnet. In the finite-doping case, $\langle d_i^\dagger d_i\rangle = 1-\delta$, the optimal $\mathbf{q}$ must vary with the hole density δ because the t term favors $\mathbf{q}=0$ as seen in Eq. (4). In the following we investigate two types of spiral phases; diagonal ($q_x = q_y = q$) and stripe ($q_x = \pi$, $q_y = q$) (see Fig. 1). In the diagonal phase, the t term becomes

$$H_t = -\frac{8}{3}tS^2C_qC_{q/2}\sum_{\mathbf{k}}(C_{k_x}+C_{k_y})d_{\mathbf{k}}^\dagger d_{\mathbf{k}}. \tag{5}$$

When $\delta \ll 1$, we can assume $q \lesssim \pi$ and $C_qC_{q/2} < 0$. Hence d particles occupy the corners of the first Brillouin zone and d holes are located around $\mathbf{k}=\mathbf{0}$. Note that we are working in the rotated frame. When transformed back to the original frame, the electron operator c can be written in terms of d as follows:

$$c_{i\uparrow} = d\cos(\mathbf{q}\cdot\mathbf{r}_i/2),$$
$$c_{i\downarrow} = -d\sin(\mathbf{q}\cdot\mathbf{r}_i/2),$$

and in momentum space

$$c_{\mathbf{k}\uparrow} = (d_{\mathbf{k}+\mathbf{q}/2} + d_{\mathbf{k}-\mathbf{q}/2})/2,$$
$$c_{\mathbf{k}\downarrow} = (d_{\mathbf{k}-\mathbf{q}/2} - d_{\mathbf{k}+\mathbf{q}/2})/2\text{i}.$$

This means that $d_{\mathbf{k}=\mathbf{0}}$ holes are composed of $c_{\pm\mathbf{q}/2}$ holes and therefore the doped *real* holes stay around $\mathbf{k} = \pm\mathbf{q}/2$ which is around $\pm(\pi/2,\pi/2)$. Similarly, when we choose $q_x = -q_y$, the location of doped real holes is around $\mathbf{k} = \pm(\pi/2,-\pi/2)$.

Using the exact form of the state density for the square lattice, we calculate the hopping energy for the diagonal phase with $\mathbf{q} = (q,q)$ and obtain the total energy per site $E_{\text{diag}}(q) = \langle H\rangle/N$:

$$E_{\text{diag}}(q) \simeq -\frac{16}{3}tS^2|C_qC_{q/2}|\delta + 2JS^2C_q \tag{6}$$

for $\delta \ll 1$. By analyzing this energy as a function of q, we can easily see that when $\delta < \delta_c \equiv 3(1+\sqrt{2})J/8t$ the minimum energy $E_{\text{diag}}^{\min}$ is given at

$$q = 2\cos^{-1}\frac{\sqrt{4+6(8t\delta/3J)^2}-2}{16t\delta/J}, \tag{7}$$

which is approximately given by $q = \pm\pi - (4/3)t\delta/J$ for $\delta \ll 1$, and when $\delta > \delta_c$ the energy is lowest at $q=0$. Consequently, as far as the diagonal phase is concerned, the spiral-spin structure characterized by the wave vector $q = \pm\pi-(4/3)t\delta/J$ abruptly changes into the ferromagtic order at the critical hole density δ_c.

If we choose $\mathbf{q} = (\pi, q)$ (stripe phase), we obtain the total energy for $\delta \ll 1$:

$$E_{\text{stripe}}(q) \simeq -\frac{8}{3}tS^2|C_qC_{q/2}|\delta + JS^2(C_q - 1). \tag{8}$$

E_{stripe} has a minimum $E_{\text{stripe}}^{\min}$ also at q given by Eq. (7) when $\delta < \delta_c$ and at $q=0$ when $\delta > \delta_c$. It is easily shown that $E_{\text{diagonal}}^{\min} < E_{\text{stripe}}^{\min}$. As a result, at low doping ($\delta < \delta_c$) the diagonal spiral order with wave vector q given by Eq. (7) appears upon doping, and when holes are doped beyond the critical value $3(1+\sqrt{2})J/8t$, the ferromagnetic LRO suddenly takes place. At this transition the wave vector q changes discontinuously.

There are two important points to be noted. First, the spiral wave vector q varies linearly with $t\delta/J$ as far as $\delta \ll 1$, which is a result previously obtained in several studies mentioned in Sec. I. Secondly, the wave vector q discontinuously changes at the boundary between the spiral and ferromagnetic phases. (Remember that those phases are continuously connected in the Hubbard model according to Ref. 6.) Figure 2 gives a schematic description of the phase diagram for the low-doping region. Since we have used the condition $\delta \ll 1$, we cannot see how far the ferromagnetic region extends in the moderate doping, although it is one of the important issues for the study of the t-J model.[8]

Extension to a model which contains next-nearest-neighbor hopping t' in addition to the nearest-neighbor hopping t is straightforward. We numerically calculated

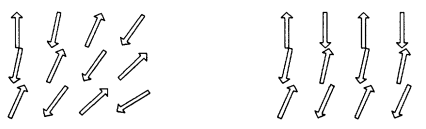

FIG. 1. Schematic illustration of the diagonal spiral phase and the stripe spiral phase. In the diagonal phase the spiral pitch is the same both in the x and y directions, and in the stripe phase it is fixed to be antiferromagnetic in one direction (x direction in this figure).

the energy of the magnetic phases and obtained the phase diagram shown in Fig. 2. We see that the, t' term stabilizes Néel order since it is associated with hopping on the same sublattice while the t term represents hopping between different sublattices.

The stability of the spiral phase against electron-density fluctuations can be easily checked. Here we show the case of the t-J model, but we get a similar result for the t-t'-J model. When $\delta \ll 1$, the t term of Eq. (4) gives $\epsilon_F \sim (16/3)tS^2|C_qC_{q/2}|(1-\pi\delta)+\mathcal{O}(\delta^2)$ and hence $\partial\epsilon_F/\partial\delta$ is positive, which means the spiral phase is unstable against density fluctuation. (Note that the Fermi energy ϵ_F is defined for particles, not for holes. Hence the derivative of ϵ_F with respect to the electron density is negative in this case.) This situation can be intuitively understood as follows. Equation (4) shows that the bandwidth is proportional to $|C_qC_{q/2}| \sim (2/3)t\delta/J$. Therefore the Fermi energy, which is a decreasing function of δ in an ordinary rigid-band model, could be raised by the expansion of the band upon doping. In addition, the constant term which comes from the J term is also an increasing function of δ in the low-doping limit. When those two contributions exceed the decrease of the electron filling, we may have $\partial\epsilon_F/\partial\delta > 0$, as in the present case.

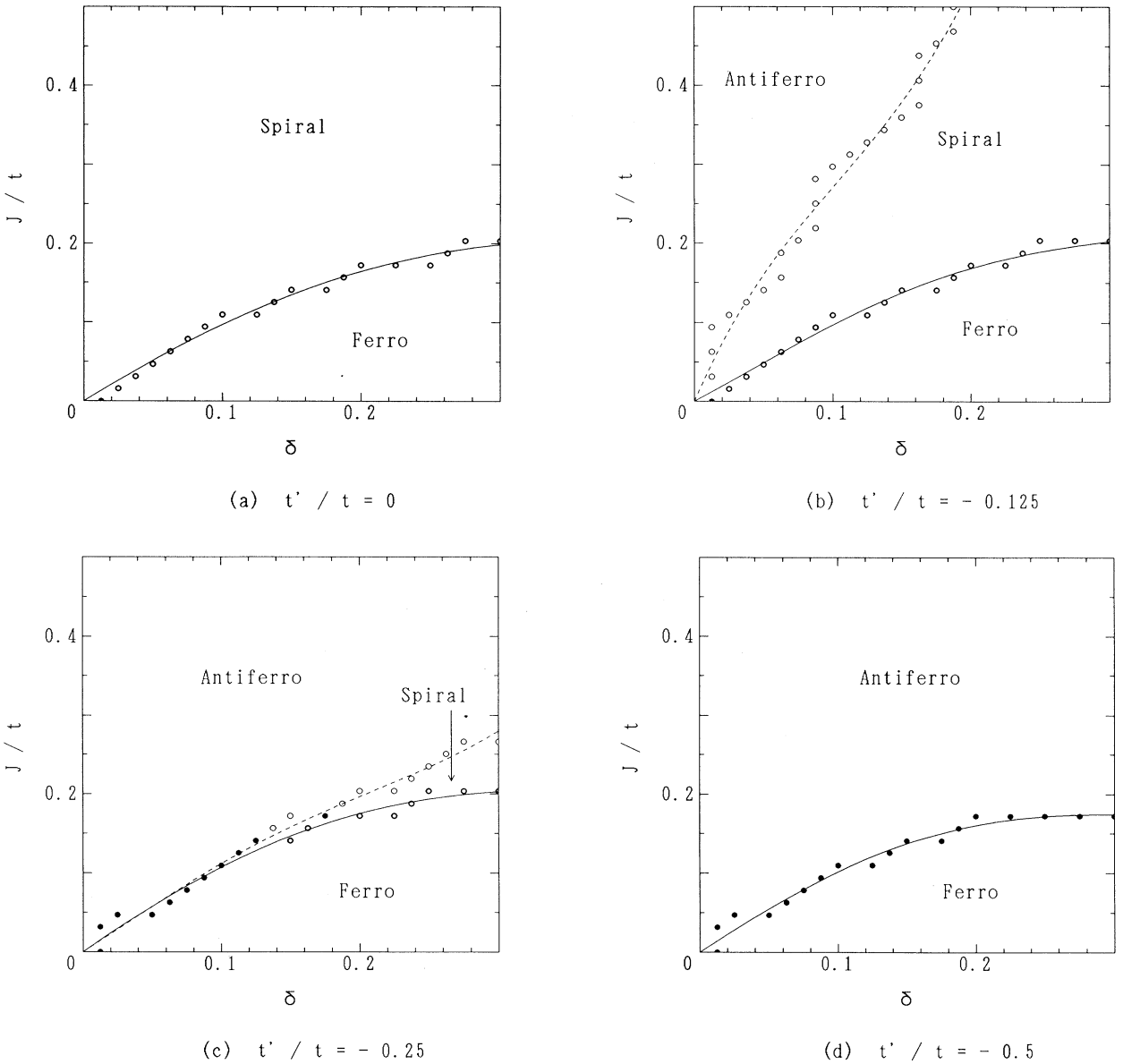

FIG. 2. Phase diagrams for the t-t'-J model obtained in the mean-field approximation in the low-doping region: (a) $t'/t = 0$, (b) $t'/t = -0.125$, (c) $t'/t = -0.25$, and (d) $t'/t = -0.5$. Here "spiral" means the diagonal spiral phase. There is a discontinuous change in the spiral pitch from finite q to $q = 0$ on the critical line between the spiral and ferromagnetic phases. The spiral phase is shown in the text to be unstable, however.

III. SPIN-WAVE EFFECT

Since the above results are obtained by the classical spin approximation, the situation could be changed by taking into account an effect of spin waves. If the spin wave induces incoherent motion of holes, the simple analysis based on the band description of holes might no longer be correct. So in what follows we investigate the spiral-spin-wave effect on the hole motion.

It is straightforward to take account of the spin fluctuations in the t-J model. Since we have assumed the spins are ferromagnetically ordered in the rotated coordinates, we make the ferromagnetic Holstein-Primakoff transformation there: $S'^{+} \simeq \sqrt{2S}b$, $S'^{-} \simeq \sqrt{2S}b^{\dagger}$, and $S'^{z} = S - b^{\dagger}b$, where $\mathbf{S}'$ is the spin operator in the rotated coordinates and b is a boson operator. The spin coupling $\mathbf{S}_i \cdot \mathbf{S}_j$ in the original frame is thus written by

$$\mathbf{S}_i \cdot \mathbf{S}_j = S^2 \cos \mathbf{q} \cdot (\mathbf{r}_i - \mathbf{r}_j) - \frac{\sqrt{2S}}{2} \sin \mathbf{q} \cdot (\mathbf{r}_i - \mathbf{r}_j) + \frac{S}{2}[\cos \mathbf{q} \cdot (\mathbf{r}_i - \mathbf{r}_j) - 1](b_i b_j + b_i^{\dagger} b_j^{\dagger}) + \frac{S}{2}[\cos \mathbf{q} \cdot (\mathbf{r}_i - \mathbf{r}_j) + 1](b_i b_j^{\dagger} + b_i^{\dagger} b_j) - S \cos \mathbf{q} \cdot (\mathbf{r}_i - \mathbf{r}_j)(b_i^{\dagger} b_i + b_j^{\dagger} b_j) + O(S^0), \tag{9}$$

and consequently the Heisenberg term becomes, in momentum space,

$$H_J = JNS^2 \gamma_{\mathbf{q}} + J\frac{S}{2} \sum_{\mathbf{k}} \mathbf{b}_{\mathbf{k}}^{\dagger} (\Delta_{\mathbf{q},\mathbf{k}} - 2\gamma_{\mathbf{q}} + \Gamma_{\mathbf{q},\mathbf{k}} \sigma_x) \mathbf{b}_{\mathbf{k}} - JS \sum_{\mathbf{k}} (\Delta_{\mathbf{q},\mathbf{k}} - 2\gamma_{\mathbf{q}}), \tag{10}$$

where

$$\Delta_{\mathbf{q},\mathbf{k}} = (C_{q_x} + 1)C_{k_x} + (C_{q_y} + 1)C_{k_y},$$
$$\gamma_{\mathbf{q}} = C_{q_x} + C_{q_y},$$
$$\Gamma_{\mathbf{q},\mathbf{k}} = (C_{q_x} - 1)C_{k_x} + (C_{q_y} - 1)C_{k_y},$$

$\mathbf{b}_{\mathbf{k}}^{\dagger} = (b_{\mathbf{k}}^{\dagger}, b_{-\mathbf{k}})$, and σ_x is the x component of Pauli matrix. Since in the large-S limit, $[d_\sigma, b] = d_{\sigma-1}/\sqrt{2S} \to 0$, we can treat the d particle and the b particle independently. Then the t term can be written in terms of d and b in the form;

$$H_t = \sum_{\mathbf{k}} \epsilon(\mathbf{q},\mathbf{k}) d_{\mathbf{k}}^{\dagger} d_{\mathbf{k}} + \sum_{\mathbf{k},\mathbf{k}'} D(\mathbf{q},\mathbf{k},\mathbf{k}') d_{\mathbf{k}}^{\dagger} d_{\mathbf{k}'} (b_{\mathbf{k}-\mathbf{k}'} + b_{\mathbf{k}'-\mathbf{k}}^{\dagger}), \tag{11}$$

where

$$\epsilon(\mathbf{q},\mathbf{k}) = -\frac{8}{3} t S^2 (C_{q_x/2} C_{q_x} C_{k_x} + C_{q_y/2} C_{q_y} C_{k_y}),$$
$$D(\mathbf{q},\mathbf{k},\mathbf{k}') = -\mathrm{i}\frac{4}{3}\sqrt{2S} S \frac{t}{\sqrt{N}} [C_{q_x/2} S_{q_x} (S_{k'_x} - S_{k_x}) + C_{q_y/2} S_{q_y} (S_{k'_y} - S_{k_y})],$$

and $S_q = \sin q$. The second term in Eq. (11) represents the emission and absorption of a spin wave due to carrier hopping. It is noted that the coupling D is small, compared with the bandwidth, since $D/t \sim O[(t\delta/J)^2]$ while $\epsilon/t \sim O(t\delta/J)$.

We calculate the self-energy of the d particle collecting noncrossing diagrams in the self-consistent Born approximation.[4,9] The nonperturbed Green's function G_0 for d particles and 2×2 matrix Green's function G_s for the two-component spin-wave operator $\mathbf{b}$ are respectively given by

$$G_0 = \{\omega - \epsilon(\mathbf{q},\mathbf{k}) + \mathrm{i}\eta \ \mathrm{sgn}[\epsilon(\mathbf{q},\mathbf{k}) - \epsilon_F]\}^{-1}, \tag{12}$$
$$G_s = \left(\omega - J\frac{S}{2}(\Delta_{\mathbf{q},\mathbf{k}} - 2\gamma_{\mathbf{q}} + \Gamma_{\mathbf{q},\mathbf{k}}\sigma_x + \mathrm{i}\eta)\right)^{-1},$$

where $\eta = +0$. The self-energy $\Sigma(\mathbf{k},\omega)$ is defined by $G^{-1} = G_0^{-1} - \Sigma$ where G is the renormalized Green's function for d particles. Σ is obtained for the diagonal phase in the self-consistent Born approximation as

$$\Sigma(\mathbf{k},\omega) = \sum_{\mathbf{k}'} |D(\mathbf{q},\mathbf{k},\mathbf{k}')|^2 G(\mathbf{k}', \omega - \omega_{\mathbf{q},\mathbf{k}-\mathbf{k}'}), \tag{13}$$

where

$$\omega_{\mathbf{q},\mathbf{k}} = JSC_q(\gamma_{\mathbf{k}} - 2). \tag{14}$$

We numerically solved Eq. (13) for the 16×16 lattice using Eq. (7). The quasiparticle energy $E_{\mathbf{k}}$ defined by

$$E_{\mathbf{k}} = \epsilon(\mathbf{q},\mathbf{k}) + \mathrm{Re}\Sigma(\mathbf{k}, E_{\mathbf{k}})$$

is given in Fig. 3 for $J = 0.25$ and $\delta = 0.05$. (Here and in all the following figures the energy unit is taken to be t. Also remember that the d particles are composed of real electrons whose momentum is different by $\pm\mathbf{q}/2$

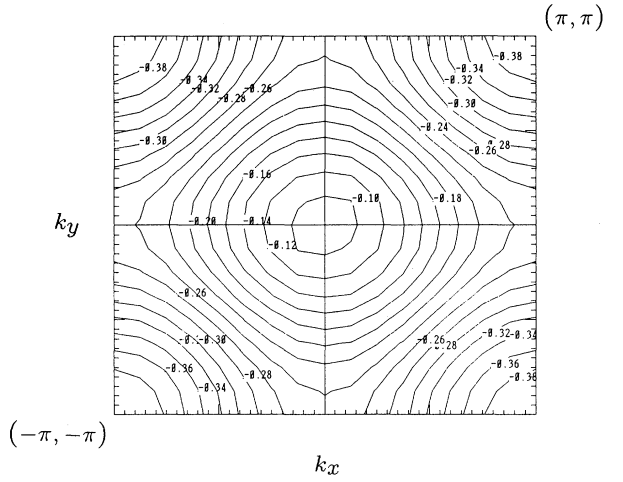

FIG. 3. The energy contour of $E_{\mathbf{k}}$, where $J = 0.25$ and $\delta = 0.05$.

from that of the d particles, and that all the analyses are made in terms of such d particles.) As clearly seen in the figure the dispersion is almost the same as the mean-field cosine band of $\epsilon(\mathbf{q},\mathbf{k})$, and the spin-wave effect coming from $\mathrm{Re}\Sigma$ seems quite small. The quasiparticle weight

$$z(\mathbf{k}) = [1 - \partial\,\mathrm{Re}\Sigma(\mathbf{k},\omega]/\partial\omega)^{-1}|_{\omega=E_{\mathbf{k}}}$$

for the same parameters as in Fig. 3 is shown in Fig. 4, where the data are plotted in the form $1-z(\mathbf{k})$. There are some values of $\mathbf{k}$ giving $z(\mathbf{k}) > 1$, which are not plotted in Fig. 4. Those are just numerical errors in a sense given below. The self-energy Σ as a function of ω generally has some structure over a certain range of ω, and the quasiparticle energy $E_{\mathbf{k}}$ is to be located in any of the following energy regions depending on the parameters we use: the low-energy side of the oscillating region of Σ, the high-energy side of that, and the oscillating region. If $E_{\mathbf{k}}$ is in the rapidly oscillating region of Σ, the numerical derivative $\partial\,\mathrm{Re}\Sigma/\partial\omega$ at $\omega = E_{\mathbf{k}}$ not only has insufficient accuracy but is significantly affected by the finite-size effect. Hence we have $z(\mathbf{k}) > 1$ when $E_{\mathbf{k}}$ happens to encounter the fine structure of $\mathrm{Re}\Sigma$. It should be stressed, however, that this is a rare situation, because Σ has a fine structure only when we choose parameters such that $E_{\mathbf{k}}$ is in the lower-energy side. For most cases, Σ tends to change

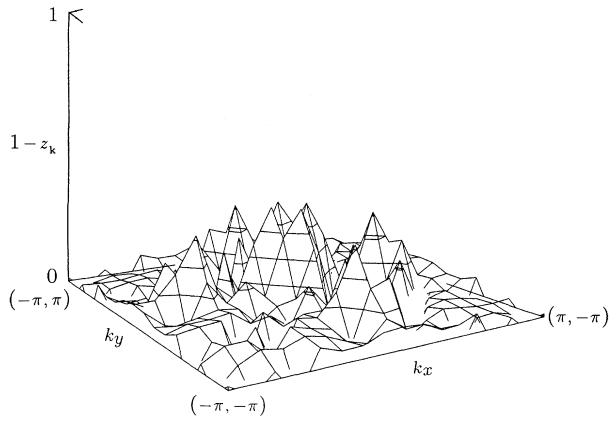

FIG. 4. The quasiparticle weight $z(\mathbf{k})$ for $J = 0.25$ and $\delta = 0.05$.

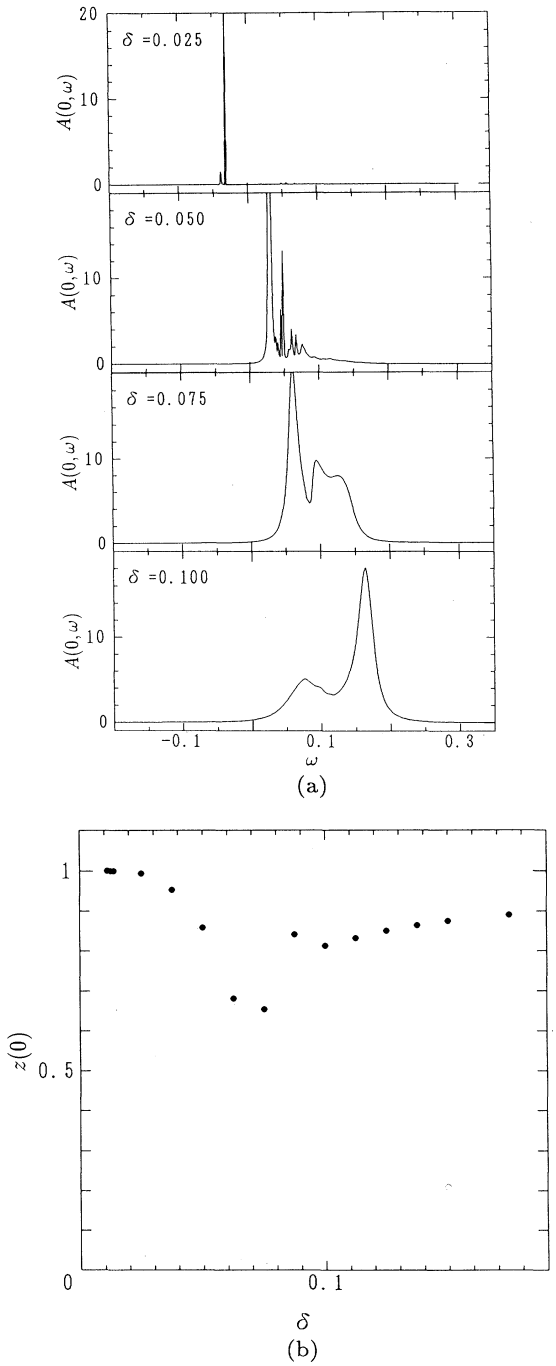

FIG. 5. (a) The spectral functions $A(\mathbf{k},\omega)$ at $\mathbf{k} = 0$ for $\delta = 0.025, 0.050, 0.075$, and 0.100 with $J = 0.25$. (b) The quasiparticle weight $z(\mathbf{k})$ at $\mathbf{k} = 0$ vs δ, where $J = 0.25$.

its shape to be more smooth as we make $E_{\mathbf{k}}$ larger using appropriate parameters, and when $E_{\mathbf{k}}$ enters it, the shape of Σ has already been smooth enough to give accurately a numerical derivative $\partial \mathrm{Re}\Sigma/\partial\omega|_{\omega=E_{\mathbf{k}}}$. However, for some $\mathbf{k}$ and some parameters, it could happen that Σ still barely keeps a fine structure even when $E_{\mathbf{k}}$ reaches the low-energy end of such structure. As for a single hole doped in the Néel background,[9] $E_{\mathbf{k}}$ is shown to always be located in the lower-energy side and the spectral function has a peak at low energy accompanying incoherent structure at higher energies.

To see more clearly this situation, let us show how the spectral function $A(\mathbf{k},\omega) = -(1/\pi)\mathrm{Im}G(\mathbf{k},\omega)$ and the self-energy $\Sigma(\mathbf{k},\omega)$ at $\mathbf{k} = \mathbf{0}$ would be changed as we vary the parameters δ and J. Figure 5(a) displays that the coherent peak moves from the low-energy side to the higher-energy side as δ increases. When δ is sufficiently small we have a coherent peak at low energy and the negligibly small incoherent structure follows in the higher-energy side. As δ increases, the higher-energy part grows and finally forms a new coherent peak. On the other hand, the coherent peak at low energy is gradually destroyed into an incoherent broad peak. For the intermediate values of δ around $\delta = 0.075$, the quasiparticle weight has a low value as shown in Fig. 5(b). In this range of the intermediate δ value the quasiparticle energy $E_{\mathbf{k}}$ stays in the oscillating region of $\mathrm{Re}\Sigma$. When we vary J instead of δ, the situation is completely reversed (Fig. 6).

The difference of those two behaviors of the spectral function in terms of δ and J is explained if we see it in terms of the spiral wave vector q. Noting that $q = \pm\pi - (4/3)t\delta/J$, we can summarize the above behaviors as follows: Near the Néel order (cf. the phase diagram in Fig. 2) a coherent peak is located at low energy, and, as we move away from the Néel ordered phase and approach the ferromagnetic region, another coherent peak grows in the high-energy side with simultaneous collapse of the low-energy peak. In other words the qualitative feature of the spectral function is determined by q rather than δ or J. This is primarily because the quasiparticle energy is almost determined by the mean-field energy $\epsilon(\mathbf{q},\mathbf{k})$ which explicitely depends on q. Since $\epsilon(\mathbf{q},\mathbf{0}) = -(16/3)tS^2C_{q/2}C_q$, $\epsilon(\mathbf{q},\mathbf{0})$ is zero at $q = \pi$ and is increased as q becomes smaller, that is, $E_{\mathbf{k}}$ is an increasing (decreasing) function of δ (J).

Although we saw some relatively small values of $z(\mathbf{k})$,

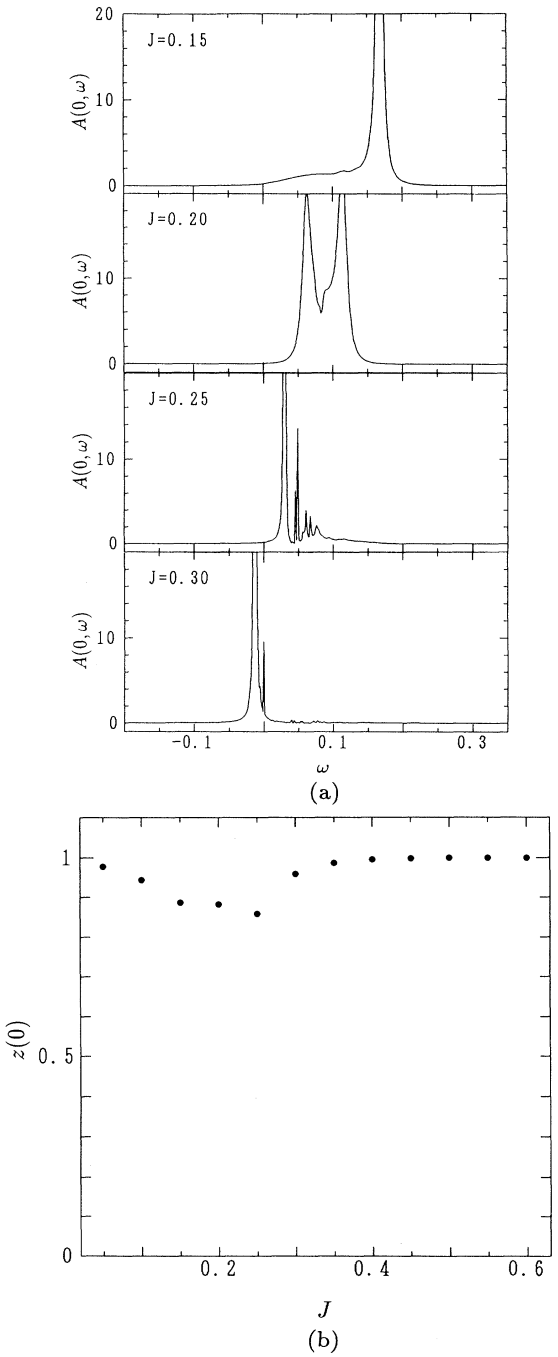

FIG. 6. (a) $A(\mathbf{k},\omega)$ at $\mathbf{k} = 0$ for $J = 0.15$, 0.20, 0.25, and 0.30 with $\delta = 0.05$. (b) $z(\mathbf{k})$ at $\mathbf{k} = 0$ as a function of J with $\delta = 0.05$.

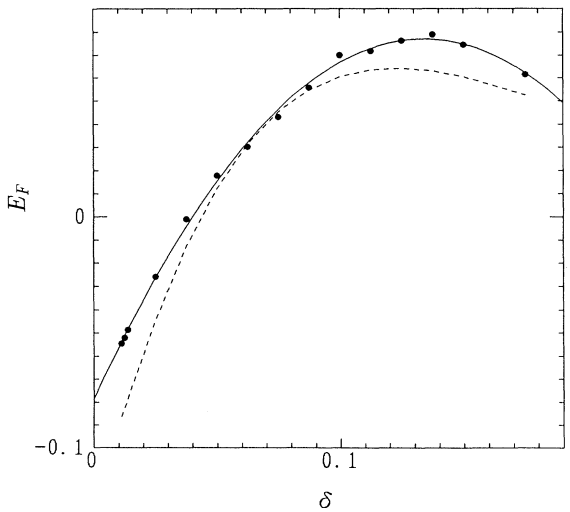

FIG. 7. The Fermi energy vs δ (solid circles). The dashed line shows the mean-field result and the solid line is a guide for the eyes.

we did not find any parameter region which gives the totally incoherent feature of the spectral function, and the band scheme of the mean-field analysis still seems to hold in the presence of the spiral-spin wave. Therefore the mean-field conclusion that the spiral phase is not stable due to density fluctuations is expected to be unchanged even if we take account of the spin-wave effect. Actually, as shown in Fig. 7 where the Fermi energy as a function of δ is plotted, we see $\partial\epsilon_F/\partial\delta > 0$ in the low-doping region. (Although in a moderate doping, $\partial\epsilon_F/\partial\delta$ becomes negative both in the mean-field result and in the perturbed result, we cannot judge whether or not the spiral phase is stable in this doping region because we have used the approximation which is valid only in the low-doping limit.)

For the finite t' model we also got similar results.

IV. SUMMARY AND DISCUSSION

In order to analyze the electron-spin interaction in the t-J model, we transform the model to the form of Eq. (2), which clearly shows the interaction. We start the analysis using this form of the t-J model. Since the new form contains the spin operators explicitly, we employed the classical spin approximation for the first step. As a result we obtained a phase diagram where the magnetic LRO varies from Néel to spiral order and the spiral pitch becomes longer as we dope. There is a critical hole density $\delta_c = 3(1+\sqrt{2})J/8t$ beyond which ferromagnetic LRO takes place. The spiral pitch discontinuously jumps at this phase boundary, in contrast to the case of the Hubbard model.[6] This spiral phase is not stable, however. The calculation of the Fermi energy shows that the system has a negative compressibility, namely the density fluctuation would spontaneously occur and the spiral phase would not be able to keep its uniformity. We also extended the model to include next-nearest-neighbor hopping t', and show the Néel phase grows with t'.

Although we do not know what kind of phase takes the place of the spiral phase, it is expected that the unknown phase has lower energy than the ferromagnetic phase and the area of the ferromagnetic phase should be smaller. Hence we consider the calculated critical density δ_c as a lower limit of the true value.

We also investigated how the spin-wave effect modifies this mean-field result. The spectral function shows a coherent peak at low energy followed by a high-energy incoherent background when the system is nearly Néel ordered. As long as we stay in the vicinity of the Néel phase, i.e., as long as $\mathbf{q} \simeq (\pi,\pi)$, the incoherent background is extremely small. As we go away from the Néel phase, however, the location of the peak moves to higher energy and simultaneously the incoherent part is gradually developed. Then a new peak appears in the incoherent background, and the lower-energy peak breaks into incoherent background as we approach the boundary between the spiral and ferromagnetic phases. Despite those features, the spectral function never becomes totally incoherent for any case, that is, the spin-fluctuation effect on the mean-field solution is not crucial. Therefore the doping dependence of the Fermi energy is qualitatively the same as that in the mean-field result, and the spiral phase, which is shown by the mean-field analysis to be unstable due to density fluctuations, would not be stabilized by the presence of the spin wave.

We should make some comments regarding the high-temperature superconductors. All those materials equally show the Néel order in a small but finite range of doping near half filling, in contrast to the present result. In our analysis for the t-J model (with no t' term) using the $S \to \infty$ approximation, the magnetic LRO is to be modified from commensurate Néel to spiral order as we dope, because the doped holes cannot move in the classical rigid Néel background but can propagate smoothly in the spiral background. The magnetic background tends to change its form losing some magnetic energy in order to gain the kinetic energy of doped holes. There can be at least two possible scenarios for the stabilization of the Néel order in the finite doping region, however. One is the presence of the next-nearest-neighbor hopping, which is shown in the above to stabilize Néel order. The second is the spin-fluctuation effect. Since we have quantum spins and not classical spins, the spin-flipping process removes traces which doped holes leave behind. So we might have a finite area for the Néel phase even in the t-J model. Actually a high-temperature expansion[10] indicates that Néel order remains in a finite range of doping.

ACKNOWLEDGMENTS

The authors would like to thank Professor K. Machida and Dr. H. Shimahara for fruitful discussions.

* On leave from Department of Materials Science, Faculty of Science, Hiroshima University, Higashi-Hiroshima 724, Japan.

[1] B.I. Shraiman and E.D. Siggia, Phys. Rev. Lett. **62**, 1564 (1989).
[2] C.L. Kane *et al.*, Phys. Rev. B **41**, 2653 (1990).
[3] A. Auerbach and B.E. Larson, Phys. Rev. B **43**, 7800 (1991).
[4] J. Igarashi and P. Fulde, Phys. Rev. B **45**, 10 419 (1992); **45**, 12 357 (1992).
[5] M. Kato *et al.*, J. Phys. Soc. Jpn. **59**, 1047 (1990); Z.Y. Weng, Phys. Rev. Lett. **66**, 2156 (1991); S. Sarker, Phys. Rev. B **43**, 8775 (1991); S. John and P. Voruganti, *ibid.* **43**, 10 815 (1991); E. Arrigoni and G.C. Strinati, *ibid.* **44**, 7455 (1991).
[6] H.J. Schultz, Phys. Rev. Lett. **65**, 2462 (1990).
[7] J.H. Xu *et al.*, Phys. Rev. B **43**, 8733 (1991).
[8] For example, see W.O. Puttika, M.U. Luchini, and T.M. Rice, Phys. Rev. Lett. **68**, 538 (1992); W.O. Puttika, M.U. Luchini, and M. Ogata, *ibid.* **69**, 2288 (1992).
[9] C.L. Kane *et al.*, Phys. Rev. B **39**, 6880 (1989); S. Schmitt-Rink *et al.*, Phys. Rev. Lett. **60**, 2793 (1988); F. Marsiglio *et al.*, Phys. Rev. B **43**, 10 882 (1991); Z. Liu and E. Manousakis, *ibid.* **45**, 2425 (1992).
[10] R.R.P. Singh and R.L. Glenister, Phys. Rev. B **46**, 11 871 (1992).